IJE TRANSACTIONS A: Basics Vol. 39, No. 10, (October 2026) 2602-2616

International Journal of Engineering

Journal Homepage: www.ije.ir

Optimal Design of Excitation Inputs for Identifying the Dynamics of Fixed-wing Aircraft Considering Active Control in MIMO Systems

A. Mohseni[a], M. Mortazavi*[b], N. Sayyaf[a], S. A. Askari[a]

[a] *Department of Mechanical Engineering, University of Isfahan, Isfahan, Iran*
[b] *Department of Electrical Engineering, University of Isfahan, Isfahan, Iran*

PAPER INFO

Paper history:
Received 16 September 2025
Received in revised form 25 October 2025
Accepted 08 January 2026

Keywords:
Aircraft
System Identification
Excitation Input Design
Parameter Estimation
Multi-input Multi-output Systems
Closed Loop

ABSTRACT

This study presents a systematic and optimal framework for designing excitation inputs for fixed-wing aircraft system identification, with a particular focus on multi-input multi-output (MIMO) systems under active flight control. Excitation signals such as pulse, doublet, and multi-step are commonly selected due to their simplicity and widespread use in practical applications. However, their selection is often empirical and may not provide optimal excitation for accurate and robust parameter estimation. The proposed methodology systematically determines the most effective input signals, designs their frequency content and amplitude characteristics, and evaluates their performance under both open- and closed-loop control conditions. This approach facilitates accurate parameter estimation across multiple identification techniques and is generalizable to other aircraft as well as potentially to other complex dynamic systems. The effectiveness of the proposed method is demonstrated through high-fidelity six-degree-of-freedom (6-DOF) simulations in MATLAB/Simulink, showing its capability to efficiently and accurately excite the relevant aircraft modes for precise model identification.

doi: *10.5829/ije.2026.39.10a.20*

Graphical Abstract

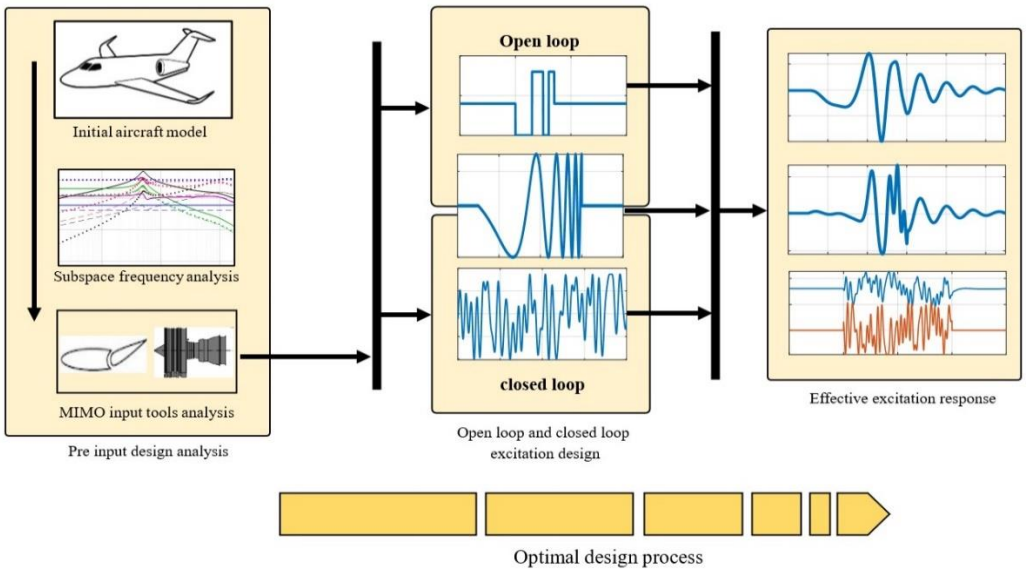

*Corresponding Author Email: ma.mortazavi@eng.ui.ac.ir (M. Mortazavi)

Please cite this article as: Mohseni A, Mortazavi M, Sayyaf N, Askari SA. Optimal Design of Excitation Inputs for Identifying the Dynamics of Fixed-wing Aircraft Considering Active Control in MIMO Systems. International Journal of Engineering, Transactions A: Basics. 2026;39(10):2602-16.

1. INTRODUCTION

System identification is a fundamental discipline that has consistently played a pivotal role in the design and development of aerospace vehicles, with enduring applications from historical projects to contemporary advanced aircraft. This methodology is employed across a diverse spectrum of areas, including understanding and optimizing aircraft behavior, designing and refining control systems, fault detection and diagnosis, developing high-fidelity simulators, establishing handling qualities criteria, and planning efficient aerial missions (1-5). A core tenet of system identification is that flight data must be rich in information about the dynamic characteristics to be identified; as a fundamental rule, "if the characteristics are not in the data, do not expect to be able to identify them in the model" (6). Consequently, the design of appropriate excitation inputs to stimulate the aircraft's dynamics during flight tests, — thereby ensuring the collection of informative data— represents one of the most critical stages in the identification process. This design must be executed systematically and aligned precisely with the objectives of the system identification endeavor.

The most prevalent excitation inputs in aircraft system identification include pulse, doublet, multi-step, sinusoidal, and multi-sinusoidal signals, each serving specific purposes (7-10). For instance, the doublet and multi-step inputs are widely utilized due to their simplicity and effectiveness in exciting a desired frequency range, making them particularly suitable for identifying short-period and Dutch roll modes (11-14). Conversely, the pulse input is more appropriate for exciting and characterizing the phugoid mode (15, 16). Another commonly used input is the frequency sweep, which covers a broad range of frequencies and is especially valuable when prior knowledge of the system dynamics is limited (17, 18). Among more recent developments, the Orthogonal Optimized Multisine (OOM) method (7) has been introduced as a practical, versatile, and effective approach for flight test applications. It has been employed both theoretically and experimentally for the excitation of aircraft dynamics and the estimation of dynamic parameters (19, 20). Given their predominant application in exciting aircraft system dynamics, these input types form the primary focus of the present investigation.

In Multi-Input Multi-Output (MIMO) systems, a crucial consideration is determining the impact of different control effectors on the identification process. For example, in an aircraft featuring a V-tail configuration, longitudinal dynamics can be excited using the elevator, rudder, or engine thrust. A review of the existing literature reveals that excitation inputs are often designed and applied based on traditional or empirical methods, frequently leading to suboptimal performance and increased time and cost for flight testing and identification (21-23). While these references address input design for identifying aircraft dynamics, the critical questions of how to apply these inputs across multiple channels and their subsequent effects are often not thoroughly examined. Furthermore, besides the application strategy, key input characteristics—such as frequency content, amplitude, duration, and signal shape—must be meticulously designed with respect to the specific aircraft dynamics. This aspect of tailored input design has also been largely overlooked in favor of more conventional approaches .

Another critical factor in aircraft system identification is the state of the flight control system, which can be either active or inactive, corresponding to closed-loop or open-loop identification, respectively. In open-loop identification, the control system is disengaged, allowing excitation inputs to be applied directly to the aircraft, stimulating its dynamics according to the input's frequency content. However, for most modern aircraft, mission requirements and safety constraints often preclude open-loop operation due to their reliance on active stability augmentation and flight control systems. Consequently, the active controller significantly influences the system's response to excitations, making open-loop identification challenging and often impractical (4, 24, 25). While necessary, closed-loop testing introduces specific challenges; primarily, the feedback control action can dampen the excitation signals and introduce correlations between the control input and process noise, complicating the identification process (4). Under these conditions, excitation inputs must be designed to optimally overcome these limitations and effectively excite the system dynamics, a challenge that is addressed in this work.

System identification and precise dynamic modeling, in addition to the mathematical model and flight motion equations, have novel applications in other parts of an aircraft as well. Recent advancements in UAV-based sensing and control systems highlight the growing importance of precise dynamic modeling and identification for complex aerial platforms. For example, reference (26) developed a UAV-based structural health monitoring system combining vision-based localization and deep learning models to detect structural defects in GNSS-denied environments. Similarly, Jiang et al. (27) integrated intelligent sensors with UAVs to enhance operational safety and spatial awareness. These studies underscore the increasing reliance on UAVs as intelligent dynamic systems that require accurate system identification and effective input design, motivating the development of the systematic framework proposed in this work.

Despite the variety of existing methods for designing excitation inputs, a persistent challenge in aircraft system

identification is their optimal design, particularly when multiple control effectors are involved and the control system is active. Flight testing is inherently risky, costly, and time-consuming. Therefore, it is imperative to design excitation inputs purposefully and efficiently to maximize information yield and minimize the number of required test flights. Most existing studies focus on specific excitation types or single-input cases and do not provide a unified procedure for evaluating and comparing their effectiveness under different flight conditions. To further clarify the importance of this topic, Table 1 lists some studies that have employed excitation inputs, along with the identified design limitations.

The main contribution of this paper is to present a systematic and optimal framework for designing and evaluating excitation inputs for fixed-wing aircraft. The method accounts for both open- and closed-loop conditions in MIMO systems. In this context, the proposed process not only determines suitable excitation frequency ranges but also evaluates which control effectors (e.g., elevator or throttle) are more effective for exciting specific aircraft modes and extracting aerodynamic derivatives. The novelty of this work lies in addressing all key challenges simultaneously — including the closed-loop nature of the system, the MIMO interactions between control effectors, and the difficulty of properly exciting relevant modes while maintaining safe flight conditions. The proposed framework provides an integrated process that can be applied to various aircraft configurations and potentially extended to other dynamic systems.

The paper is structured as follows: the first section details the derivation of the initial aircraft model. The second section presents the design of the excitation frequency range based on this model and provides a method for selecting the most effective input in MIMO systems. The third section develops various excitation inputs according to the specified frequency range and analyzes their performance through simulation. The fourth section addresses the specific design of excitation inputs for closed-loop system identification. Finally, the fifth section designs an optimal excitation input for the target aircraft and validates its effectiveness through comprehensive six-degree-of-freedom (6-DOF) simulations in the MATLAB/Simulink environment.

2. DERIVATION OF INITIAL MODEL

The design process for excitation inputs begins with the development of a mathematical model representing the system at its intended operational condition. Following this approach, the longitudinal state-space model of the fixed-wing aircraft is formulated according to Equation 1. (28).

$$\begin{cases} \dot{x} = Ax + Bu_{inp} \\ y = Cx + Du_{inp} \end{cases}, \tag{1}$$

Where matrices A and B are defined as follows:

$$A = \begin{bmatrix} X_u + X_{Tu} + \frac{X_{\dot{\alpha}}(Z_u + Z_{Tu})}{U_1 - Z_{\dot{\alpha}}} & X_\alpha + \frac{X_{\dot{\alpha}} Z_\alpha}{U_1 - Z_{\dot{\alpha}}} & X_q + \frac{X_{\dot{\alpha}}(U_1 + Z_q)}{U_1 - Z_{\dot{\alpha}}} & -g \\ \frac{Z_u + Z_{Tu}}{U_1 - Z_{\dot{\alpha}}} & \frac{Z_\alpha}{U_1 - Z_{\dot{\alpha}}} & \frac{U_1 + Z_q}{U_1 - Z_{\dot{\alpha}}} & 0 \\ M_u + M_{Tu} + \frac{M_{\dot{\alpha}}(Z_u + Z_{Tu})}{U_1 - Z_{\dot{\alpha}}} & M_\alpha + M_{T\alpha} + \frac{M_{\dot{\alpha}} Z_\alpha}{U_1 - Z_{\dot{\alpha}}} & M_q + M_{\dot{\alpha}} + \frac{U_1 + Z_q}{U_1 - Z_{\dot{\alpha}}} & 0 \\ 0 & 0 & 1 & 0 \end{bmatrix} \tag{2}$$

$$B = \begin{bmatrix} X_{\delta e} + \frac{X_{\dot{\alpha}} Z_{\delta e}}{U_1 - Z_{\dot{\alpha}}} & X_T + \frac{X_{\dot{\alpha}} Z_T}{U_1 - Z_{\dot{\alpha}}} \\ \frac{Z_{\delta e}}{U_1 - Z_{\dot{\alpha}}} & \frac{Z_T}{U_1 - Z_{\dot{\alpha}}} \\ M_{\delta e} + \frac{M_{\dot{\alpha}} Z_{\delta e}}{U_1 - Z_{\dot{\alpha}}} & M_T + \frac{M_{\dot{\alpha}} Z_T}{U_1 - Z_{\dot{\alpha}}} \\ 0 & 0 \end{bmatrix} \tag{3}$$

TABLE 1. Comparison of issues in the design of excitation inputs in selected references

Refs.	Input type	Closed loop excitation	Optimal Control Effector in MIMO	Frequency range estimation	Optimal process
(1)	MS	*	*	*	*
(4)	FS	✓	*	*	*
(7)	OOM	*	*	✓	*
(8)	OOM 3211	*	*	✓	*
(9, 11)	D 3211	*	*	*	*
(12, 14)	MS OOM	✓	*	✓	*
(15)	OOM MS	✓	*	✓	*
(19)	OOM	✓	*	✓	*

D: Doublet, FS: Frequency sweep, MS: Multi sign

Also, the states vector $x = [u \quad \alpha \quad q \quad \theta]$ denotes longitudinal speed, angle of attack, pitch rate and flight pitch angle respectively. The control inputs $u_{inp} = [\delta e \ \ \delta_{th}]$ represent elevator and throttle. For simplifying, the matrix A and B in Equations 2 and 3 are expressed as Equations 4 and 5, respectively. This simplification is accepted for aircraft dynamics and is documented in reputable aerospace references (29, 30), as the effect of the omitted terms is negligible compared to the retained terms. Since the objective is to determine the effects of aerodynamic terms on the forces and moments applied to the aircraft and their respective frequency ranges, this simplification provides an appropriate approximation of each term independently.

$$A_{simplified} = \begin{bmatrix} X_u & X_\alpha & X_q & -g \\ \frac{Z_u}{U_1} & \frac{Z_\alpha}{U_1} & 1 & 0 \\ M_u & M_\alpha & M_q & 0 \\ 0 & 0 & 1 & 0 \end{bmatrix} \quad (4)$$

$$B_{simplified} = \begin{bmatrix} X_{\delta e} & X_T \\ Z_{\delta e} & Z_T \\ M_{\delta e} & M_T \\ 0 & 0 \end{bmatrix} \quad (5)$$

The coefficients in the aforementioned equations can be estimated through computational fluid dynamics (CFD) analysis (31, 32), wind tunnel testing (33, 34), or empirical methods such as DATCOM and vortex lattice methods like AVL (35-38). Although these techniques provide initial estimates for the system parameters, the resulting values often lack the precision required for high-fidelity modeling. The primary objective of system identification is to refine these parameter estimates accurately by leveraging flight test data. To this end, excitation inputs must be strategically designed and applied to ensure the system response comprehensively captures the relevant dynamic modes. This is achieved by utilizing the initial model to calculate the magnitude of these dynamic terms across the frequency range of interest. In the present study, longitudinal data from a scaled model of a Bonanza fixed-wing aircraft is employed. The key specifications of the aircraft under trim conditions are summarized in Table 2.

TABLE 2. Bonanza scale model aircraft reference data

Parameter	Value	Unit
Mass	8.5	Kg
Wing span	2.9	M
Wing area	0.55	M^2
Mean aerodynamic chord	0.19	M
Trim altitude (MSL)	2000	M
Trim speed (U1)	25	m/s

Hence, Equations 6 to 8 provide the values of the state-space matrices A and B and the aircraft dynamic mode poles, where sp and ph denote short period and phugoid modes respectively. In this study, these values were obtained using the DATCOM method, which provides an initial approximation of the model. This approximation is suitable for initial estimating the desired frequency range for exciting the aircraft modes.

$$A = \begin{bmatrix} -0.1107 & 4.1015 & 0 & -9.8 \\ -0.0312 & -4.5948 & 0.9695 & 0 \\ 0.0360 & -74.927 & -5.370 & 0 \\ 0 & 0 & 1 & 0 \end{bmatrix} \quad (6)$$

$$B = \begin{bmatrix} -0.2747 & 0 \\ -0.1052 & 0 \\ -28.9236 & -0.094 \\ 0 & 0 \end{bmatrix} \quad (7)$$

$$\begin{cases} s_{1.2} = -4.99 \pm 8.51 \, , \zeta_{sp} = 0.5 \ , \omega_{n_{sp}} = 9.87 \frac{rad}{s} \\ s_{3.4} = -0.047 \pm 5.0 \, , \zeta_{ph} = 0.09 \, , \omega_{n_{ph}} = 0.5 \frac{rad}{s} \end{cases} \quad (8)$$

3. CALCULATION OF DESIRED FREQUENCY RANGE

The design of excitation inputs for system identification and parameter estimation of fixed-wing aircraft follows a systematic three-stage methodology. The initial stage involves determining the frequency range essential for accurate parameter estimation. In the second stage, the most effective control surfaces (inputs) for exciting the aircraft's dynamics are selected. The final stage entails synthesizing specific excitation signals that adequately cover the designated frequency bandwidth. The target frequency range is determined by analyzing the contribution of each aerodynamic parameter to the force and moment equations. This analysis is performed using Bode diagrams, which pinpoint the frequency bands where the influence of each parameter is most observable. This ensures that the designed excitation inputs effectively target these critical frequencies. Furthermore, comparative analysis of Bode diagrams across different control inputs facilitates the selection of the optimal input channel for estimating each specific parameter. The frequency response of each state-space parameter is calculated using the transfer function approach outlined in Equation 9. For example, for the parameter M_α, the magnitude of the term $\left|(M_\alpha \alpha) \ / \ u_{inp}\right|$ is computed accordingly (39).

$$\begin{cases} y = \alpha = Cx + Du \\ \alpha = [0\ 1\ 0\ 0] * [u\ \alpha\ q\ \theta]' + [0\ 0] * [\delta e\ T] \\ M_\alpha \alpha = [0\ M_\alpha\ 0\ 0] * x + [0\ 0] * u_{inp} \\ C = [0\ A(3.3)\ 0\ 0] = [0\ M_\alpha\ 0\ 0] \\ D = [0\ 0] \end{cases} \quad (9)$$

So, the $\left|M_\alpha \alpha / u_{inp}\right|$ can be calculated using space state:

$$\left|M_\alpha \alpha / u_{inp}\right| = |C(SI - A)^{-1}B + D| \quad (10)$$

Which A and B matrices has been presented in Equations 2 to 7. It is worth noting that Equation 10 can be calculated using (ss2tf(A, B, C, D)) in MATLAB. Also, the term A12=$M_\alpha + M_{T\alpha} + \frac{M_{\dot{\alpha}} Z_\alpha}{U_1 - Z_{\dot{\alpha}}}$ is simplified as M_α.

Similar to Equations 9 and 10, the magnitude of the terms corresponding to other state-space parameters is calculated in the same manner as Table 3.

The frequency responses of the parameter magnitudes for both control inputs—the elevator and engine thrust—are presented in the Bode diagram shown in Figure 1. In this figure, input 1(In(1)) corresponds to the elevator input, and input 2 (In(2)) corresponds to the engine throttle. It should be noted that the frequency range determined in Figure 1, corresponds to the elements of the state-space matrix A. For example, the element A_{33} comprises the sum of $M_q + M_\alpha$. These terms must be separated and distinguished post-identification using mathematical methods.

TABLE 3. State-Space Representation for Individual Parameter Effects

Row	Parameter	Simplified	C Matrix	D Matrix
1	$\left\|\frac{\dot{u}}{u_{inp}}\right\|$	$\left\|\frac{\dot{u}}{u_{inp}}\right\|$	$[A_{11}\ A_{12}\ A_{13}\ A_{14}]$	$[B_{11}\ B_{12}]$
2	$\left\|\frac{A_{11}u}{u_{inp}}\right\|$	$\left\|\frac{X_u u}{u_{inp}}\right\|$	$[A_{11}\ 0\ 0\ 0]$	$[0\ 0]$
3	$\left\|\frac{A_{12}\alpha}{u_{inp}}\right\|$	$\left\|\frac{X_\alpha \alpha}{u_{inp}}\right\|$	$[0\ A_{12}\ 0\ 0]$	$[0\ 0]$
4	$\left\|\frac{A_{13}q}{u_{inp}}\right\|$	$\left\|\frac{X_q q}{u_{inp}}\right\|$	$[0\ 0\ A_{13}\ 0]$	$[0\ 0]$
5	$\left\|\frac{B_{11}u_{inp}}{u_{inp}}\right\|$	$\|X_{\delta e}\|$	$[0\ 0\ 0\ 0]$	$[B_{11}\ 0]$
6	$\left\|\frac{\dot{\alpha}}{u_{inp}}\right\|$	$\left\|\frac{\dot{\alpha}}{u_{inp}}\right\|$	$[A_{21}\ A_{22}\ A_{23}\ A_{24}]$	$[B_{21}\ B_{22}]$
7	$\left\|\frac{A_{21}u}{u_{inp}}\right\|$	$\left\|\frac{Z_u u}{u_{inp}}\right\|$	$[A_{21}\ 0\ 0\ 0]$	$[0\ 0]$
8	$\left\|\frac{A_{22}\alpha}{u_{inp}}\right\|$	$\left\|\frac{Z_\alpha \alpha}{u_{inp}}\right\|$	$[0\ A_{22}\ 0\ 0]$	$[0\ 0]$
9	$\left\|\frac{A_{23}q}{u_{inp}}\right\|$	$\left\|\frac{Z_q q}{u_{inp}}\right\|$	$[0\ 0\ A_{23}\ 0]$	$[0\ 0]$
10	$\left\|\frac{B_{21}u_{inp}}{u_{inp}}\right\|$	$\|Z_{\delta e}\|$	$[0\ 0\ 0\ 0]$	$[B_{21}\ 0]$
11	$\left\|\frac{\dot{q}}{u_{inp}}\right\|$	$\left\|\frac{\dot{q}}{u_{inp}}\right\|$	$[A_{31}\ A_{32}\ A_{33}\ A_{34}]$	$[B_{31}\ B_{32}]$
12	$\left\|\frac{A_{31}u}{u_{inp}}\right\|$	$\left\|\frac{M_u u}{u_{inp}}\right\|$	$[A_{31}\ 0\ 0\ 0]$	$[0\ 0]$
13	$\left\|\frac{A_{32}\alpha}{u_{inp}}\right\|$	$\left\|\frac{M_\alpha \alpha}{u_{inp}}\right\|$	$[0\ A_{32}\ 0\ 0]$	$[0\ 0]$
14	$\left\|\frac{A_{33}q}{u_{inp}}\right\|$	$\left\|\frac{M_q q}{u_{inp}}\right\|$	$[0\ 0\ A_{33}\ 0]$	$[0\ 0]$
15	$\left\|\frac{B_{31}u_{inp}}{u_{inp}}\right\|$	$\|X_{\delta e}\|$	$[0\ 0\ 0\ 0]$	$[B_{31}\ 0]$
16	$\left\|\frac{B_{32}u_{inp}}{u_{inp}}\right\|$	$\|M_T\|$	$[0\ 0\ 0\ 0]$	$[0\ B_{32}]$

When parameters exhibit overlapping magnitudes in a Bode magnitude plot, their differentiation becomes challenging. In such cases, phase plots provide a powerful complementary tool for discrimination, as they often reveal unique phase behaviors—such as distinct phase shifts or steep phase slopes near natural frequencies—that are characteristic of individual parameters. By synergistically combining both magnitude and phase information, a unique dynamic signature for each parameter can be established, greatly aiding the identification process. However, challenges persist when parameters exhibit similar phase characteristics or when phase measurements are corrupted by noise. Under these conditions, the application of advanced techniques, such as modal analysis or time-domain parameter estimation, becomes necessary. Employing high-resolution frequency data alongside sophisticated computational tools can further enhance the accuracy and reliability of parameter differentiation.

As evidenced by the Bode diagram in Figure 1, the optimal frequency range for parameter estimation can be effectively determined. A comparison of the parameter magnitudes in response to elevator versus throttle inputs reveals that the elevator generates significantly larger magnitudes across key parameters. This indicates the superior effectiveness of the elevator for exciting the system dynamics and achieving accurate parameter identification.

Furthermore, it is observed that certain parameters, such as specific control derivatives, exhibit inherently small magnitudes, rendering them more challenging to identify.

The frequency spectrum can be partitioned into two distinct regions corresponding to the aircraft's short-period and phugoid (long-period) dynamic modes (Equation 8). Consequently, the elevator has been selected as the primary control input for excitation, and the target frequency range for input design is determined to be 0.1 to 10 rad/s (base on Figure 1), as summarized in Table 4.

4. EXCITATION INPUT

The primary function of an excitation input is to actively perturb the aircraft's dynamic modes. To ensure effective and safe excitation, the input must be designed to maintain the aircraft within a linear range around its trim conditions. This requirement implies that the input amplitude must remain within predefined limits, and the input signal must begin and end at the trim value to avoid introducing a net change in the aircraft's state.

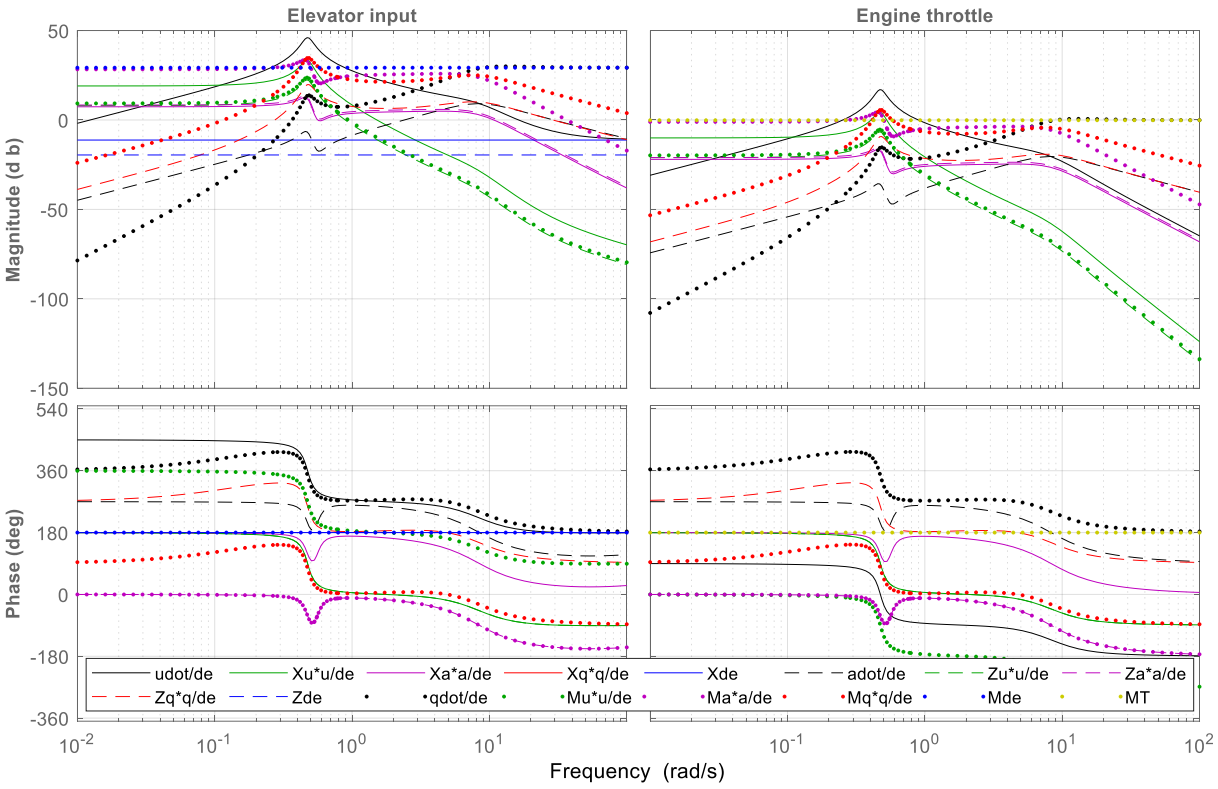

Figure 1. Frequency Response (Magnitude & Phase) of Individual Parameters for Different Control Inputs

TABLE 4. Determining frequency range for aircraft dynamic excitation

Parameter	Simplified	Frequency range (rad/s)
A_{11}	X_u	0.1 to 0.7
A_{12}	X_α	0.1 to 10
A_{13}	X_q	---
A_{21}	Z_u	0.1 to 0.5
A_{22}	Z_α	0.1 to 10
A_{23}	Z_q	0.2 to 10
A_{31}	M_u	0.1 to 0.7
A_{32}	M_α	0.2 to 10
A_{33}	M_q	0.2 to 10
B_{31}	$M_{\delta e}$	All frequency Range
$A_{11}.A_{21}.A_{31}$	$X_u.Z_u.M_u$	Phugoid: 0.1 to 0.7
$A_{12}.A_{22}.A_{23}.$ $A_{32}.A_{33}$	$X_\alpha.Z_\alpha.Z_q.$ $M_\alpha.M_q$	Short period: 8 to 10

Consequently, a conventional step input is generally unsuitable for flight test applications due to its persistent offset. Alternative signals, synthesized from combinations of pulse functions—such as pulse, doublet, and multi-step inputs—are employed instead. It is critical that the selected input possesses sufficient energy spectral density across the targeted frequency band to adequately excite the relevant system dynamics. For inputs derived from pulse combinations, the total energy of the signal can be quantified using Equation 11 (39).

$$E(w) = \frac{2\Delta t^2(1-\cos\Omega)}{\Omega^2}\left[\sum_{i=1}^{N} V_i^2 + 2\sum_{j=1}^{N-1}\cos j\Omega \sum_{i=1}^{N-j} V_i V_{i+j}\right]. \quad \Omega > 0 \tag{11}$$

where $\Omega = \omega\Delta t$ is the normalized frequency, $T = N\Delta t$ is the total duration of the input consisting of N impulses each of duration Δt, and V_i is the amplitude for the current impulse. Consequently, for each input, the energy versus frequency graph is plotted to determine which input provides suitable energy within the desired frequency range. Based on an established empirical criterion, the frequency band over which the signal's energy exceeds 50% of its maximum value can be defined as the effectively excited frequency range (39).

The amplitude and the time interval Δt for an input can be determined based on the load factor applied to the aircraft and the deviation from trim conditions. The load factor should not exceed the allowable limit specified in the aircraft flight manual. Additionally, the applied excitation should not drive the aircraft's flight conditions significantly away from the pre-excitation state. In this

study, these considerations have been evaluated through simulation, and accordingly, the amplitude and time interval have been appropriately limited.

4. 1. Pulse Input A pulse input is one of the simplest and effective excitation signals used in aircraft system identification. By applying a short-duration control surface deflection, the aircraft dynamics are excited over a frequency range, allowing the transient response to reveal information about the underlying aerodynamic and stability derivatives. This method is particularly attractive due to its ease of implementation during flight tests and its ability to provide data for parameter estimation with minimal pilot workload. The pulse input is illustrated in Figure 2. To design this input, two parameters, Δt and amplitude A, must be determined. In Figure 2, the energy of this input is shown for different A and Δt values.

The amplitude of the excitation input must be constrained to a range that prevents significant deviation from trim conditions and ensures the resulting load factor remains within acceptable structural and safety limits. Simulation results for a pulse input with a duration of $\Delta t = 1.2$ s and an amplitude of $A = 0.2$ radians are presented in Figure 3. It is evident that employing a larger input amplitude induces a higher load factor and causes substantial deviation from the nominal trim condition. The Power Spectral Density (PSD) analysis in Figure 3 indicates that the pulse input is particularly suitable for exciting low-frequency dynamics, such as the phugoid mode. Furthermore, the total energy of the pulse input, calculated from the aircraft's pitch rate response, is 19.11 $(\text{rad/s})^2$. Each figure consists of six subplots, arranged in 3 rows and 2 columns. The first row, first column shows the aircraft velocity in meters per second; the first row, second column shows the pitch rate in degrees per second; the second row, first column depicts the load factor applied to the aircraft; the second row, second column illustrates the aircraft pitch angle in degrees; the third row, first column shows the signal energy or power spectral density across different frequencies; and the third row, second column represents the input applied to the aircraft. The inputs are applied starting from the 10th second, with the aircraft trimmed during the initial 10 seconds. The data prior to this period are not shown for clarity.

4. 2. Doublet Input A doublet input is constructed by summing two consecutive pulse signals. This input waveform, along with its spectral energy distribution for a specific amplitude and time step, is illustrated in Figure 4. The horizontal axis represents the normalized frequency, ωΔt, which renders the plot dimensionless and independent of the specific time step value.

In Figure 4, the analysis focuses on the solid curves (Amplitude = 0.2 rad). Applying the previously mentioned empirical criterion, a suitable effective frequency range is identified from approximately 1.5 to 3.5 rad/s. This relationship can be expressed as:

$$\omega\Delta t = 1.5 \rightarrow \Delta t = \frac{1.5}{\omega}$$
$$\omega\Delta t = 3.5 \rightarrow \Delta t = \frac{3.5}{\omega} \quad (12)$$

Analysis of the initial model indicates a short-period natural frequency of approximately 10 rad/s and a phugoid frequency near 0.5 rad/s. Consequently, the required Δt values for effective mode excitation range from 0.15 s to 0.35 s for the short-period mode, and from 3 s to 7 s for the phugoid mode. Δt values smaller than 0.5 s produce insufficient energy magnitude in the spectral plot and fail to excite the dynamics adequately.

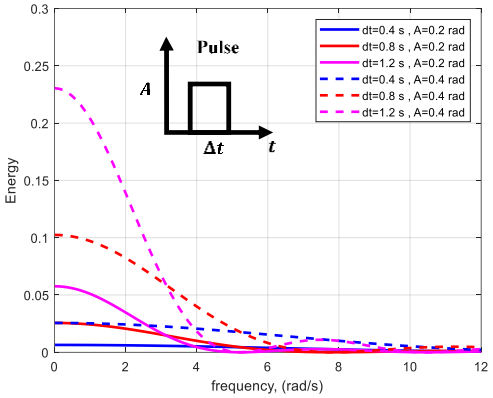

Figure 2. Pulse input and its energy across the frequency range for various Δt and A

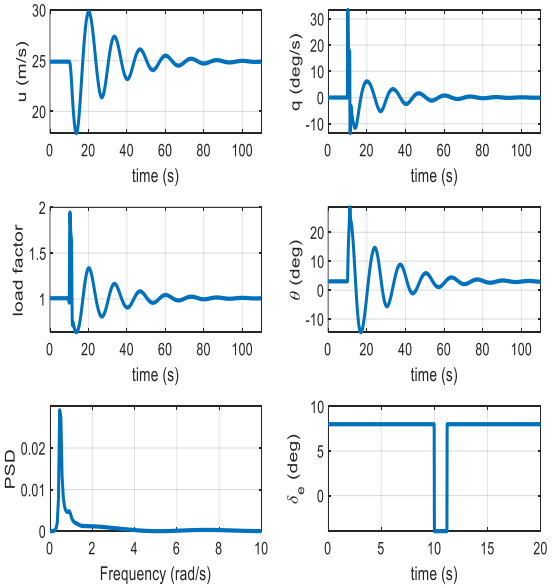

Figure 3. Pulse input (Δt=1.2 sec. and A=0.2 rad) and the aircraft response

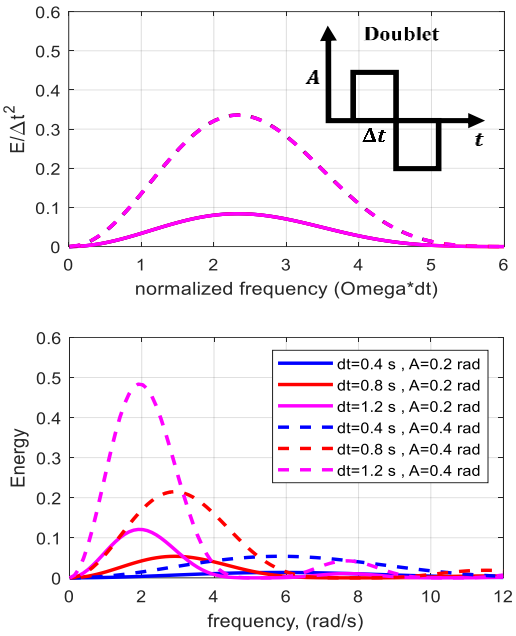

Figure 4. Doublet input and its energy across the frequency range for various Δt and A

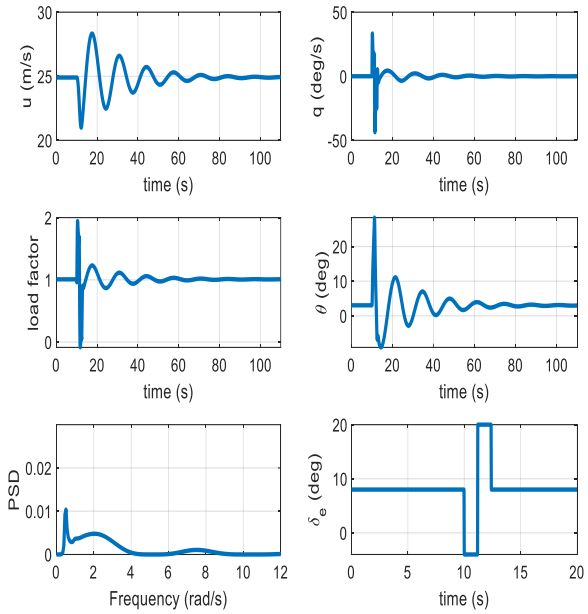

Figure 5. Doublet input (Δt=1.2 sec. and A=0.2 rad) and the aircraft response

Excessively large Δt values, conversely, cause significant deviations from trim conditions. Simulation results in Figure 5 suggest an optimal compromise at $\Delta t \approx 1.2$ s, which effectively excites frequencies in the 1 to 3 rad/s range. This makes the doublet input suitable for this specific bandwidth, though it lacks the capability to excite the short-period mode for this particular aircraft. According to Table 4, however, it remains applicable for estimating certain phugoid mode parameters. The total energy of the doublet input in Figure 5, calculated from the aircraft pitch rate response, is 27.17 $(rad/s)^2$.

4. 3. Multi Step The multi-step input is synthesized from a sequence of multiple pulse signals. The most prevalent variant is the 3211 input, which integrates both positive and negative pulses. In contrast to simple pulse and doublet inputs, this waveform is designed to excite a broader frequency spectrum. Figure 6 presents this input signal alongside its corresponding energy distribution for various amplitudes and time steps (Δt).

Consistent with the methodology applied to the doublet input in the previous section, the effective frequency range for the 3211 input is defined by the bandwidth where its normalized energy exceeds 50% of its maximum value. Analysis indicates that this corresponds to a normalized frequency (ωΔt) range of approximately 0.3 to 2.7. Consequently, by identifying the target frequency (ω) for excitation, the appropriate time step (Δt) can be systematically determined.

Numerous combinations of amplitude and Δt for the 3211 input were investigated through simulation.

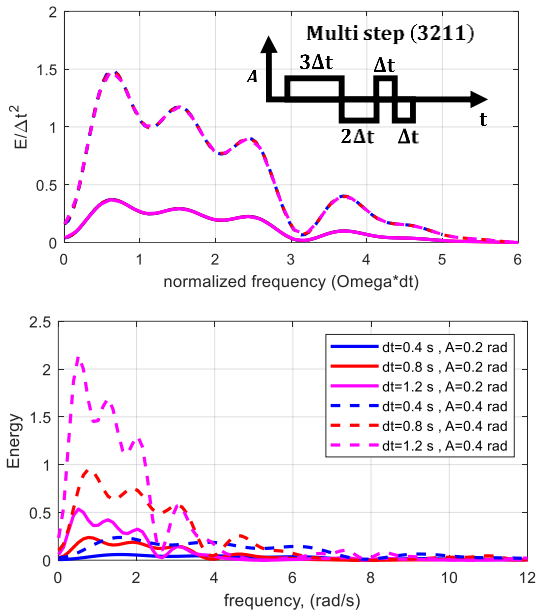

Figure 6. Multi step input and its energy across the frequency range for various Δt and A

Considering amplitude constraints inherent to flight testing, a configuration with an amplitude of 8 degrees and $\Delta t = 1\,s$ was selected for implementation. The application results of this specific input to the aircraft are depicted in Figure 7. The results demonstrate that while this input excites a wider frequency range compared to simpler inputs, the energy amplitude across this spectrum

remains relatively low. For the specific aircraft configuration in this study, the 3211 input proved ineffective in exciting the short-period mode, primarily exciting frequencies below 5 rad/s. The total energy of the multi-step input in Figure 7, calculated from the aircraft's pitch rate response, is 47.22 (rad/s)^2.

4. 4. Frequency Sweep The frequency-sweep technique is extensively employed to excite an aircraft's dynamic response across a broad frequency spectrum. This method utilizes a continuous input signal, typically a sinusoid with a linearly or exponentially varying frequency over time, facilitating the comprehensive identification and analysis of key dynamic characteristics, including natural frequencies and damping ratios. Frequency-sweep excitation is particularly advantageous when preliminary information regarding the aircraft's dynamics is limited or unavailable. The mathematical formulation for the frequency-sweep input is given by (6):

$$\begin{cases} u_{sweep} = Asin(\theta(t)) \\ \theta(t) \equiv \int_0^T \omega(t)dt \\ \omega = \omega_{min} + K(\omega_{max} - \omega_{min}) \\ K = C_2\left[\exp\left(\frac{C_1 t}{T}\right) - 1\right] \end{cases} \quad (13)$$

where ω_{min}, ω_{max} and T denote the minimum frequency, maximum frequency and total excitation duration, respectively. The values $C_1 = 4.0$ and $C_2 = 0.0187$ have been established as suitable for a wide range of applications (6). The time-history of the frequency-sweep input for a duration of $T = 50\ s$ and a frequency range from 0.3 to 12 rad/s is illustrated in Figure 8.

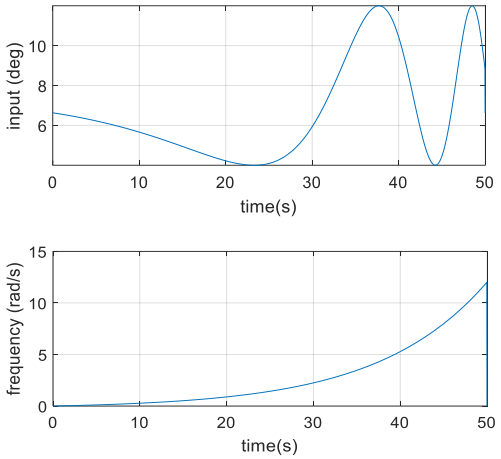

Figure 8. Frequency sweep input and its frequency progress

The system response to the applied frequency-sweep input (Figure 8) is presented in Figure 9. A primary limitation of this method is the constraint on input amplitude, which must be restricted to prevent significant deviation from trim conditions. For the specific aircraft configuration in this study, the resulting excitation amplitude across the frequency spectrum was found to be insufficient for robust identification of all modes. Consequently, while the input excites a wide frequency band, the energy distribution is not adequate for high-quality parameter estimation, particularly for modes requiring stronger excitation. The total energy of the frequency-sweep input in Figure 9, computed from the aircraft's pitch rate response, is 31.30 (rad/s)^2.

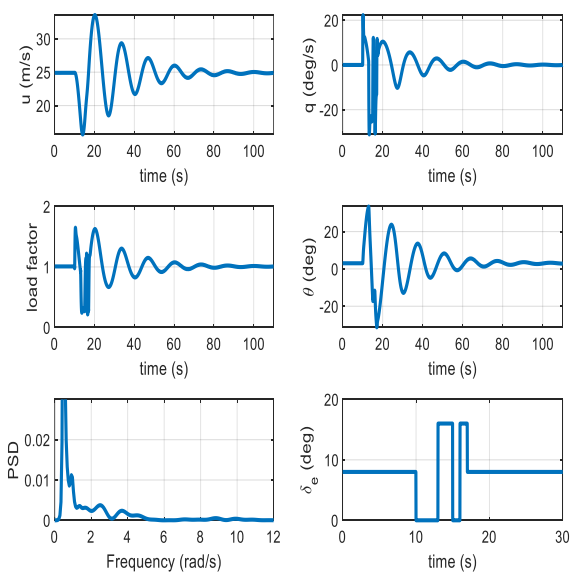

Figure 7. 3211 input (Δt=1 sec. and A=0.14 rad) and the aircraft response

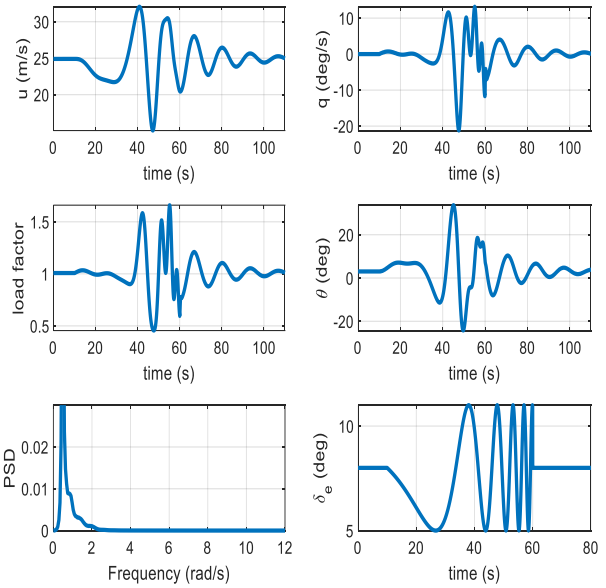

Figure 9. Frequency sweep input (T=50 sec and A=0.0524 rad) and the aircraft response

4. 5. Orthogonal Optimized Multisine Morelli (7) introduced an Orthogonal Optimized Multisine (OOM) input is. The authors claim that this input can be employed without significant operational limitations during flight and effectively excites the desired frequency range. This signal can be superimposed as a disturbance on the control surfaces while maintaining the aircraft near its trim conditions. Further comprehensive details regarding its formulation are provided by Morelli (7). The design equation for this input is given by Equation 14:

$$u = \sum_{k\in 1.2.....M} A\sqrt{P_k}\sin\left(\frac{2\pi kt}{T}+\phi_k\right) \quad (14)$$

where M is the total number of available harmonic frequencies, T is the excitation time length, A is the multisine amplitude, P_k is the power fraction for the kth sinusoidal component, and t is the time vector. The frequency $\omega_M = 2\pi M/T$ defines the upper limit of the excitation frequency band, and $\omega_1 = 2\pi/T$ defines the lower limit. In general, the superposition of harmonic components can result in large amplitude excursions, which is undesirable as it may displace the aircraft from its reference flight condition. To mitigate this, the phase angles ϕ_k in Equation 14 are optimized to minimize the Relative Peak Factor (RPF), defined as follows (7).

$$RPF(u) = \frac{[\max(u)-\min(u)]}{2\sqrt{2}\,rms(u)} \quad (15)$$

The optimal RPF value is unity. Based on Figure 1 and Table 4, a frequency range of [0.3, 10] rad/s with $T = 20\,s$ was utilized. The phase angles ϕ_k for RPF minimization were computed using a genetic algorithm. Specific details of the designed excitation input are summarized in Table 5.

The designed input signal and its frequency spectrum are shown in Figure 10. The aircraft's response to this input is presented in Figure 11. The excitation signal was combined with the elevator control input to form the total command. The total energy of the OOM input in Figure 11, calculated from the aircraft's pitch rate response, is 21.89 (rad/s)^2.

It is observed that this input successfully excites the target frequency range. Unlike conventional inputs, the OOM input enables more optimal excitation across various frequencies. Furthermore, the excitation level can be enhanced by increasing the input amplitude without necessarily compromising trim conditions.

TABLE 5. Elevator excitation input specification

A (deg)	P_k	k	$\phi_k(rad)$	$\omega(r/s)$	RPF
6	0.1	1	-3.626	0.3142	1.2
		4	3.202	1.2566	
		8	6.033	2.5133	
		11	2.911	3.4558	
		15	4.724	4.7124	
		18	0.4512	5.6549	
		22	-0.1469	6.9115	
		25	1.735	7.8540	
		29	-0.2262	9.1106	
		32	-2.035	10.053	

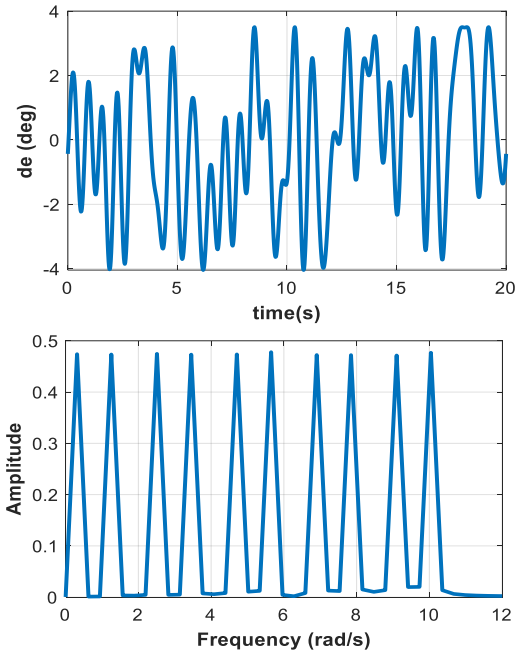

Figure 10. Designed input signal and its specific frequency

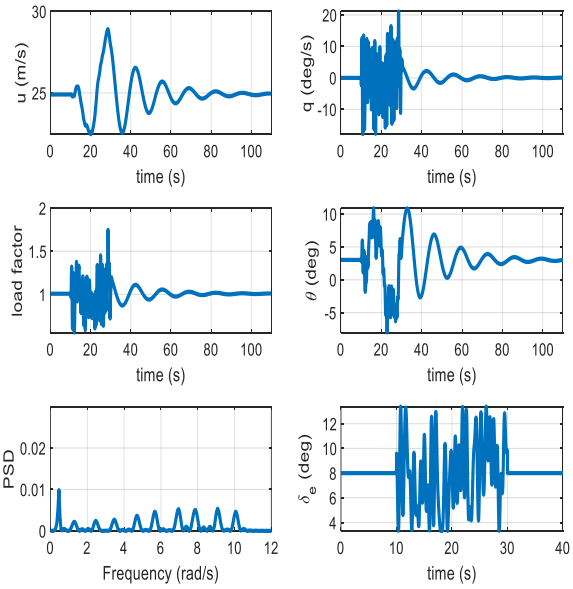

Figure 11. OOM input (T=20 sec and A=0.07 rad) and the aircraft response

As observed in this section, under open-loop excitation, all input signals are capable of stimulating the aircraft dynamics; however, the OOM, 3211, and frequency sweep inputs can excite a wider frequency range. Among these, the OOM input provides a more optimal response, as it effectively excites higher frequencies and the short-period mode.

5. CLOSED LOOP SYSTEM EXCITATION

The investigations presented thus far have focused on exciting the aircraft in open-loop configuration, without considering the presence of stability augmentation or flight control systems. However, for many modern aircraft, mission profiles and operational requirements necessitate the continuous engagement of control systems during flight. Under these conditions, the active controller significantly alters the effective excitation inputs commanded to the aircraft. In Figures 12a to 12c, the inputs designed in the previous sections are applied to the aircraft with an active control system. The results demonstrate the controller's effect on the inputs. Pulse and doublet inputs have little impact, as they are easily damped and ineffective at exciting the closed-loop system, especially at higher frequencies. Since the multi-step input encompasses these signals, only the multi-step, sinusoidal, and OOM inputs were analyzed.

One established method to mitigate the controller's influence is to inject the excitation signal directly to the control surfaces, bypassing the closed-loop controller; this technique is referred to as Surface Servo Excitation (SSE). An alternative approach involves reducing the controller gains. For the purposes of this study, the SSE method has been employed.

Analysis of the results indicates that the control system's attenuation effect diminishes as the input frequency increases. Among the tested inputs, the Orthogonal Optimized Multisine (OOM) input exhibits the greatest robustness to controller interference. Furthermore, transformation of the controller-affected OOM input into the Fourier domain confirms that higher-frequency components remain effectively excited. This demonstrates the OOM input's superior performance in closed-loop identification scenarios.

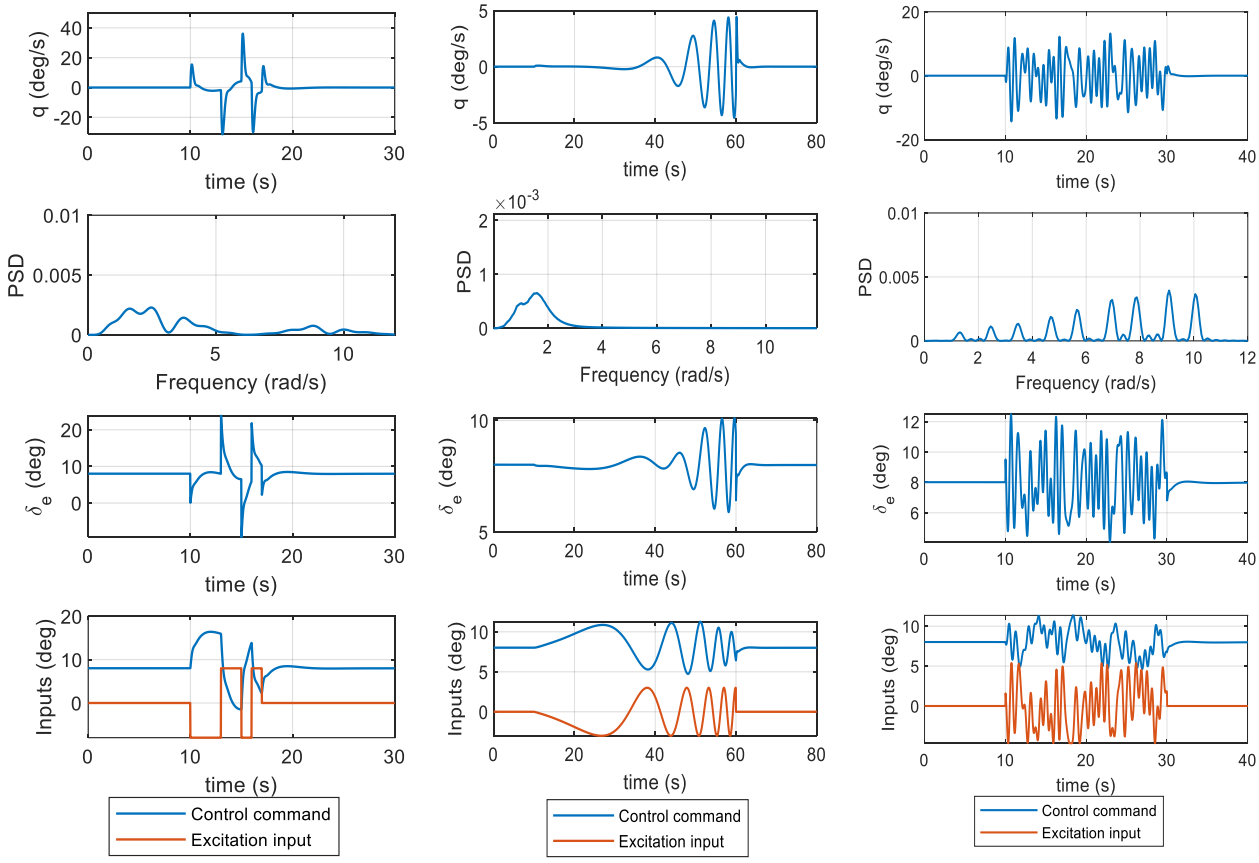

(a) Closed loop aircraft response to 3211 excitations

(b) Closed loop aircraft response to frequency sweep excitation

(c) Closed loop aircraft response to OOM excitation

Figure 12. Closed loop aircraft response to various excitation inputs

A comparative summary of the excitation inputs investigated in this article is presented in Table 6. To facilitate a quantitative comparison, a performance indices system ranging from 0, 5 and 10 is utilized, where a score of 10 indicates full satisfaction of a criterion, and a score of 0 denotes a failure to meet it. A score of 5 means the criterion is acceptable but needs some improvements or additional review.

This scoring is based on the simulation results, the capability of the input signals to excite the aircraft dynamics, and the targeted excitation range shown Figure 1. For example, as illustrated in Figure 4, the doublet input is capable of exciting the frequency up to 3.5 rad/s, which is suitable for stimulating the phugoid mode of the considered aircraft (Figure 1). This behavior is also demonstrated in the simulation results presented in Figure 5; therefore, a score of 10 has been assigned to this case.

As the table shows, the OOM input scores higher overall than the other inputs, demonstrating its superiority. It should be noted that the OOM input cannot be applied manually by a pilot and must instead be computationally pre-programmed and injected into the system automatically.

It is important to note that the results presented in this study are specific to the aircraft configuration investigated. In this paper, an optimal process for excitation input design has been developed and implemented for the aircraft under study. Although the obtained numerical results are not directly applicable to other aircraft, the proposed input design process itself has a general and adaptable structure that can be utilized for different airframes. To apply this approach to another aircraft, the steps described in Sections 2 and 3 should first be performed for the target aircraft to derive its corresponding mathematical model and to determine the desired frequency range to be excited. Then, the same optimization-based procedure introduced in this paper can be followed to design the excitation inputs. Naturally, the numerical outcomes will differ depending on the aircraft's characteristics; however, the optimal procedure for input design remains identical.

TABLE 6. Comparison of the types of excitation inputs for considered aircraft

Criteria	Pulse	Doublet	Multi step	Frequency sweep	OOM
Phugoid excitation capability	10	10	10	10	10
Short period excitation capability	0	0	5	5	10
Open loop excitation	10	10	10	10	10
Closed loop excitation	0	0	5	10*	10
Appling continuously during flight**	0	0	0	0	10
Ease of the use	10	10	10	5	5

* Just in high frequencies
** base on reference (7)

6. CONCLUSION

This study proposed a systematic and optimized framework for designing excitation inputs for longitudinal system identification of a fixed-wing MIMO aircraft under both open-loop and closed-loop configurations. A scaled Bonanza aircraft was used as the test case, and several excitation signals—pulse, doublet, multi-step, frequency sweep, and Orthogonal Optimized Multisine (OOM)—were evaluated through high-fidelity MATLAB/Simulink simulations to identify the most effective input strategy.

Results show that multi-step and OOM inputs provide the best excitation performance, yielding the most accurate identification of longitudinal dynamics while minimizing flight test effort. Frequency-domain analysis confirmed that the elevator input is more effective than the throttle for exciting longitudinal modes; thus, all final tests were performed using elevator actuation.

Based on the simulation results, experimental observations, and supporting literature, the following Practical recommendations are proposed:

- The findings presented here are specific to the aircraft configuration studied. The design process should be repeated tailored to each unique aircraft system.
- Excitation inputs should ideally be designed to initially induce a pitch-up motion.
- The exact time-domain form of the input is not critical. Minor asymmetries during manual application may even be beneficial in certain cases.
- All inputs must be applied around trimmed flight conditions. It is recommended to allow a 10-second trim period before and after each input application.
- The OOM input can be superimposed as a small-amplitude disturbance during closed-loop operation for continuous excitation, provided its amplitude remains within safe limits.
- Based on the comprehensive analysis, the use of OOM and multi-step inputs is strongly recommended for the subject aircraft. In particular, the OOM input proves highly suitable for closed-loop identification

7. FUTURE WORK

In this paper, the process of designing aircraft excitation signals for MIMO, nonlinear, opened-loop and closed-loop systems was discussed, along with the main criteria that should be considered. In future work, we intend to develop an intelligent and automated framework that can perform this process autonomously based on the defined objective. The proposed intelligent system will evaluate performance indices and automatically design the optimal excitation input according to the target identification goal.

Acknowledgements

The author appreciates Department of Mechanical Engineering, University of Isfahan for providing necessary facilities to conduct present research.

Funding

This work was supported by Aviation Research and Education Center (AREC), Department of Aerospace Engineering, University of Isfahan, Isfahan, Iran.

Ethics Approval and Consent to Participate

This article does not involve any studies with human participants or animals performed by any of the authors. Therefore, ethics approval and consent to participate are not applicable.

Competing Interests

The author declares no financial or organizational conflicts of interest.

Data Availability

The data that support the findings of this study are available upon reasonable request.

Declaration of Generative AI and AI-Assisted Technologies in the Writing Process

During the preparation of this manuscript, the author used ChatGPT and Grok exclusively for minor language editing to improve readability. After using this tool, the author carefully reviewed and edited the content as needed and takes full responsibility for the content of the published article.

Authors Biosketches

Mahdi Mortazavi is an Associate Professor in the Department of Aerospace Engineering, Faculty of Engineering, University of Isfahan. He received his Ph.D. in Aerospace Engineering from the Moscow Aviation Institute (MAI), Russia. His research interests include flight mechanics, control, guidance, and navigation.

Negin Sayyaf is an Assistant Professor in the Department of Electrical Engineering, Faculty of Engineering, University of Isfahan. She received her Ph.D. in control engineering from Sharif University of Technology. Her research interests include reinforcement learning, deep learning and artificial intelligence.

Seyed Abdorreza Askari is an Adjunct Professor at the Faculty of Engineering, University of Isfahan. He received his degree in Aerospace Engineering from Amirkabir University of Technology. His research interests include Flight mechanics and control.

Abdollah Mohseni is a Ph.D. candidate in Mechanical Engineering in the Department of Mechanical Engineering, University of Isfahan. His research interests include artificial intelligence, Flight mechanics and control, and system identification.

REFERENCES

1. Ayyad A, Chehadeh M, Awad MI, Zweiri Y. Real-time system identification using deep learning for linear processes with application to unmanned aerial vehicles. IEEE Access. 2020;8:122539-53. https://doi.org/10.1109/ACCESS.2020.3006277.
2. Belge E, Kaba H, Parlak A, Altan A, Hacıoğlu R. Estimation of small unmanned aerial vehicle lateral dynamic model with system identification approaches. Balkan Journal of Electrical and Computer Engineering. 2020;8(2):121-6. https://doi.org/10.17694/bajece.654499.
3. Hosseini B, Steinert A, Hofmann R, Fang X, Steffensen R, Holzapfel F, et al. Advancements in the theory and practice of flight vehicle system identification. Journal of Aircraft. 2023;60(5):1419-36. https://doi.org/10.2514/1.C037269.
4. Matt JJ, Chao H, Shawon MH, Svoboda BC, Hagerott SG. System Identification for Small Flying-Wing Unmanned Aircraft Using Open-Loop and Closed-Loop Flight Data. Journal of Aircraft. 2025:1-17. https://doi.org/10.2514/1.C038147.
5. Morelli EA, Klein V. Aircraft System Identification: Theory and Practice: Sunflyte Enterprises; 2016. https://doi.org/10.1017/S0001924000087194.
6. Tischler MB, Remple RK. Aircraft and rotorcraft system identification: American Institute of Aeronautics and Astronautics Reston; 2012. https://doi.org/10.2514/4.868207.
7. Morelli EA. Practical aspects of multiple-input design for aircraft system identification flight tests. AIAA Aviation 2021 Forum. https://doi.org/10.2514/6.2021-2795.
8. Lichota P, Ohme P, Sibilski K. Simultaneous multi-step excitations for aircraft system identification. AIAA Atmospheric Flight Mechanics Conference; 2016. https://doi.org/10.2514/6.2016-3704.
9. Gim H, Lee B, Huh J, Kim S, Suk J. Longitudinal system identification of an avian-type UAV considering characteristics of actuator. International Journal of Aeronautical and Space Sciences. 2018;19:1017-26. https://doi.org/10.1007/s42405-018-0084-5.

10. Aslandoğan OH. Development of a Rotorcraft Time Domain System Identification Software: Middle East Technical University (Turkey); 2023. https://hdl.handle.net/11511/101957.
11. Han Y, Kim Y. Optimal input design for online parameter estimation for aircraft with multiple control surfaces. Engineering Optimization. 2011;43(5):559-80. https://doi.org/10.1080/0305215X.2010.502937.
12. Gresham JL, Simmons BM, Fahmi J-MW, Woolsey CA. Remote uncorrelated pilot inputs for nonlinear aerodynamic model identification from flight data. AIAA Aviation 2021 Forum. https://doi.org/10.2514/6.2021-2792.
13. Fu J, Huang J, Song L, Yang D. Experimental study of aircraft achieving dutch roll mode stability without weathercock stability. International Journal of Aerospace Engineering. 2020;2020(1):8971275. https://doi.org/10.1155/2020/8971275.
14. Gresham JL, Simmons BM, Fahmi J-MW, Hopwood JW, Woolsey CA. Remote Uncorrelated Pilot Input Excitation Assessment for Unmanned Aircraft Aerodynamic Modeling. Journal of Aircraft. 2023;60(3):955-67. https://doi.org/10.2514/1.C036942.
15. Roeser MS, Fezans N. Method for designing multi-input system identification signals using a compact time-frequency representation. CEAS Aeronautical Journal. 2021;12(2):291-306. https://doi.org/10.1007/s13272-021-00499-6.
16. Kapeel EH, Safwat E, Kamel AM, Khalil MK, Elhalwagy YZ, Hendy H. Physical modeling, simulation and validation of small fixed-wing UAV. Unmanned Systems. 2023;11(04):327-50. https://doi.org/10.1142/S2301385023500152.
17. Tischler MB. System identification methods for aircraft flight control development and validation. Advances in aircraft flight control.2018:35-69. https://doi.org/10.21949/1403895.
18. Grauer JA, Boucher MJ. Aircraft system identification from multisine inputs and frequency responses. Journal of Guidance, Control, and Dynamics. 2020;43(12):2391-8. https://doi.org/10.2514/1.G005131.
19. Morelli EA. Optimal input design for aircraft stability and control flight testing. Journal of Optimization Theory and Applications. 2021;191(2):415-39. https://doi.org/10.1007/s10957-021-01912-0.
20. Hosseini S, Hofmann R, Holzapfel F, Rauleder J. Optimal Input Design for Aircraft Parameter Estimation-Flight Test Results. AIAA SCITECH 2025 Forum; 2025. https://doi.org/10.2514/6.2025-2173.
21. Lichota P. Multi-Axis Inputs for Identification of a Reconfigurable Fixed-Wing UAV. Aerospace. 2020;7(8):113. https://doi.org/10.3390/aerospace7080113.
22. Millidere M. Optimal input design and system identification for an agile aircraft: Middle East Technical University (Turkey); 2021. https://hdl.handle.net/11511/93115.
23. Mazhar MF, Wasim M, Abbas M, Riaz J, Swati RF. Aircraft system identification using multi-stage PRBS optimal inputs and maximum likelihood estimator. Aerospace. 2025;12(2):74. https://doi.org/10.3390/aerospace12020074.
24. Simsek O, Bayrak AI, Karatoprak S, Dogan A. Comparison of Open Loop and Closed Loop System Identification of a UAV. 2018 Atmospheric Flight Mechanics Conference; 2018. https://doi.org/10.2514/6.2018-3476.
25. Wang Z, Li A, Mi Y, Lu H, Wang C. Aircraft Closed-Loop Dynamic System Identification in the Entire Flight Envelope Range Based on Deep Learning. Journal of Aerospace Engineering. 2024;37(6):04024079. https://doi.org/10.1061/JAEEEZ.ASENG-5657.
26. Chu, T. S. C., Sorilla, J., & Chua, A. Y. UAV-Based Structural Health Monitoring Using a Two-Stage CNN Model with Lighthouse Localization in GNSS-Denied Environments. HighTech and Innovation Journal. 2025; 6(2), 398-410. https://doi.org/10.28991/HIJ-2025-06-02-03.
27. Jiang, Y., Pang, X., Zhang, Z., Jing, H., Wei, L., Su, J., & Zhang, P. Integrating Intelligent Sensors for Safe UAV Distribution: Design and Evaluation of Ranging System. HighTech and Innovation Journal. 2024; 5(3), 603-13. https://doi.org/10.28991/HIJ-2024-05-03-04.
28. Schmidt DK. Modern flight dynamics: McGraw-Hill New York; 2012.
29. Stevens BL, Lewis FL, Johnson EN. Aircraft control and simulation: dynamics, controls design, and autonomous systems: John Wiley & Sons; 2015. https://doi.org/10.1002/9781119174882.
30. Roskam J. Airplane flight dynamics and automatic flight controls: DARcorporation; 1998.
31. Bottigliero R, Rossano V, De Stefano G. Transonic Dynamic Stability Derivative Estimation Using Computational Fluid Dynamics: Insights from a Common Research Model. Aerospace. 2025;12(4):304. https://doi.org/10.3390/aerospace12040304.
32. Nguyen NT, Xiong J. CFD-Based Frequency Domain Method for Dynamic Stability Derivative Estimation with Application to Transonic Truss-Braced Wing. AIAA AVIATION 2022 Forum; 2022. https://doi.org/10.2514/6.2022-3596.
33. Shang T, Chen B, Yanling W, Ting Y, Hailiang L, Lixin W. Identification of aircraft longitudinal aerodynamic parameters using an online corrective test for wind tunnel virtual flight. Chinese Journal of Aeronautics. 2024;37(9):261-75. https://doi.org/10.1016/j.cja.2024.05.031.
34. Tai S, Wang L, Wang Y, Lu S, Bu C, Yue T. Identification of lateral-directional aerodynamic parameters for aircraft based on a wind tunnel virtual flight test. Aerospace. 2023;10(4):350. https://doi.org/10.3390/aerospace10040350.
35. Hassan AA-B. Calculating Aerodynamic & Stability Characteristics for Small fixed-wing UAVs based on Digital DATCOM. The International Undergraduate Research Conference; 2022: The Military Technical College. https://doi.org/10.21608/iugrc.2022.303029.
36. Ahmad M, Hussain ZL, Shah SIA, Shams TA. Estimation of stability parameters for wide body aircraft using computational techniques. Applied Sciences. 2021;11(5):2087. https://doi.org/10.3390/app11052087.
37. Granja DM. Hamiltonian Dynamics applied to aerobatic behavior of a high-performance airplane: Universidade do Porto (Portugal); 2024.
38. Rezazadeh Movahhed S, Hamed MA. Aerodynamic coefficients computation for fixed wing aircrafts using datcom software with emphasize on rudderless flying-wing uavs. Journal of Aerospace Science and Technology. 2024;17(1):60-71. https://doi.org/10.22034/jast.2023.398894.1152.
39. Jategaonkar RV. Flight vehicle system identification: a time domain methodology: American Institute of Aeronautics and Astronautics; 2006. https://doi.org/10.1017/S0001924000011015.

Persian Abstract

چکیده

در این مقاله یک چارچوب سیستماتیک و بهینه برای طراحی ورودی‌های محرک برای شناسایی سیستم هواپیماهای بال ثابت، با تمرکز ویژه بر سیستم‌های چند ورودی چند خروجی (MIMO) تحت کنترل پرواز فعال ارائه شده است. سیگنال‌های محرک مانند پالس، دابلت و چند مرحله‌ای معمولاً در شناسایی سیستم هواپیما به دلیل سادگی و کاربرد گسترده آنها انتخاب می‌شوند، نه اینکه از یک فرآیند طراحی سیستماتیک طراحی شوند. در نتیجه، انتخاب آنها اغلب تجربی است و ممکن است تحریک بهینه برای تخمین دقیق پارامتر را فراهم نکند. روش پیشنهادی به طور سیستماتیک موثرترین سیگنال‌های ورودی را تعیین می‌کند، محتوای فرکانسی آنها را طراحی می‌کند و عملکرد آنها را در هر دو شرایط حلقه باز و حلقه بسته ارزیابی می‌کند. این رویکرد تخمین دقیق پارامتر را در تکنیک‌های شناسایی متعدد تسهیل می‌کند و قابل تعمیم به سایر پیکربندی‌های هواپیما و حتی سایر سیستم‌های دینامیکی است. اثربخشی روش پیشنهادی از طریق شبیه‌سازی‌های شش درجه آزادی با دقت بالا در MATLAB/Simulink نشان داده شده است که توانایی آن را در تحریک کارآمد و دقیق حالت‌های مربوط به هواپیما برای شناسایی دقیق مدل نشان می‌دهد.